Direction of Encounter (DoE): A Mobility-Based Location Method for Wireless Networks

Michael Pascoe-Chalke, Javier Gomez-Castellanos, Veronica Bonilla-Gonzalez, Miguel Lopez-Guerrero, *Member, IEEE*, Victor Rangel-Licea, and Enrique Rodriguez-Colina, *Member, IEEE*

Abstract—Traditional location methods require specialized network infrastructure or add-on location hardware in order to estimate node positions. As an opposite approach, *direction of encounter* (DoE) uses standard wireless networking equipment and takes advantage of node mobility to establish static node locations. In DoE, as a mobile node enters and leaves a static node's coverage area, it is able to discover the static node's location with respect to its own trajectory. Mobile nodes are able to determine the position of a set of static nodes by collaborating in this discovery process. In this work, this set is called a *constellation*. This collaboration consists of exchanging *constellation* data in order to establish and improve the accuracy of the position estimates. Not only does DoE establish static node positions, but it also allows mobile users to be aware of the direction where static nodes can be found. DoE needs minimal user intervention, although fully automatic operation can be achieved if inertial sensors are available. This method can be used to develop both location-based applications and guiding procedures. By means of simulations and experiments, we carried out a performance evaluation of DoE under diverse conditions. The results show that the DoE algorithm indeed is able to estimate the static node positions without requiring additional functionality from static nodes. We believe this is an important requirement for a successful deployment of a location method.

Index Terms—Node encounter, node mobility, node detection and location

1 INTRODUCTION

In the near future, it can be foreseen that mobile nodes will be increasingly required to be able to gain access to information about their position in relation to neighboring nodes. If such information is available, mobile users may become aware of the location of other users while they are moving in a region covered by a wireless network.

The availability of location information encourages the development of *location-based services* in wireless networks. In order to operate properly, such services require a method to determine a user's position. Unfortunately, traditional location methods need specialized infrastructure or hardware in order to accurately estimate node positions. The presence of base stations or satellites with known positions, the necessity of having access to both the Internet and location services, or the use of expensive add-on hardware are some examples of this kind of requirements. Furthermore, many location algorithms are highly complex, thus demanding significant computing requirements.

In wireless networks, nodes may show some degree of mobility which has been seen as a hindering factor for location methods. However, in this work, we show that node mobility can also be used to facilitate node location. We present a method to locate static nodes by using a set of mobile nodes in a wireless network. The introduced method is infrastructure-free, i.e., it does not use GPS receivers or other location devices. This method is called direction of encounter (DoE). DoE uses standard wireless equipment and requires minimal user intervention to work. However, automatic operation is also possible if inertial sensors are available. Certainly, what makes DoE a different location approach, is that it takes advantage of node mobility to estimate static node positions. For instance, by monitoring an infrastructure-based WLAN, mobile nodes implementing DoE could discover how the access points (APs) are deployed in the network. By sharing such information with other mobile users, they could determine, for example, where to travel with the aim of getting closer to the nearest access point, thus increasing their transmission rate. In a similar way, mobile users detecting the presence of nearby nodes could use DoE to determine where to move with the purpose of finding other users.

The rest of the paper is organized as follows: Section 2 summarizes relevant works found in the literature related to location methods for wireless networks and how they interact with applications that require location information to operate. Section 3 describes how the proposed method works. Section 4 presents performance tests applied to DoE by means of simulations and experiments under a diversity of network conditions, such as a variety of node arrangements, fluctuations in the wireless transmission range due to propagation impairments and variable numbers of static and mobile nodes. Section 5 discusses a series of possible DoE applications. Finally, Section 6 provides some concluding remarks.

- *M. Pascoe-Chalke, M. Lopez-Guerrero, and E. Rodriguez-Colina are with the Department of Electrical Engineering, Metropolitan Autonomous University (UAM), Mexico City, Mexico. E-mail: {mpascoe, milo, erod}@xanum.uam.mx.*
- *J. Gomez-Castellanos, V. Rangel-Licea, and V. Bonilla-Gonzalez are with the Department of Telecommunications, National Autonomous University of Mexico (UNAM), Mexico City, Mexico. E-mail: {javierg, victor}@fi-b.unam.mx, v.bonilla@comunidad.unam.mx.*

Manuscript received 2 Mar. 2012; revised 31 Jan. 2014; accepted 2 Mar. 2014. Date of publication 16 Mar. 2014; date of current version 26 Sept. 2014. For information on obtaining reprints of this article, please send e-mail to: reprints@ieee.org, and reference the Digital Object Identifier below. Digital Object Identifier no. 10.1109/TMC.2014.2311993

2 Related Work

In this section, we summarize the most relevant works related to location methods. Over recent years, many researchers have proposed different systems designed to estimate node location in a wireless network, e.g., [1], [2], [3], [4], [5], and [6]. As suggested in several works, (e.g., [7], [8] and [9]), these systems can be classified as *range-based* or *connectivity-based* systems.

On one hand, range-based systems can be subdivided into four categories depending on which method is used to estimate or measure the distance between transmitter and receiver. These methods are based on measuring one of the following parameters: time of arrival (ToA), time-difference of arrival (TDoA), angle of arrival (AoA) and signal attenuation (SA). The value of these parameters is a function of the distance or relative position observed between a transmitter and a receiver. A location system based on ToA, e.g., [10] and [11], estimates distances by measuring the signal propagation delays between the end points of a radio link. In contrast, TDoA systems, e.g., [12], estimate the location by computing the time-difference of arrival of a signal propagating from one transmitter to three or more synchronized receivers. ToA and TDoA methods are mostly suited for communication systems where signal propagation latencies are much longer than data transmission delays, e.g., satellite or macro-cell systems. Location systems using AoA, e.g., [13], require special receivers in order to determine the angle on which radio signals arrive from a transmitter. Location systems based on SA, e.g., [14], estimate the distance between transmitters and receivers by using signal attenuation measurements. These methods involve propagation models and triangulation or lateralization techniques to estimate the node position. Radio-fingerprinting systems are based on SA methods, e.g., [3], and they operate by pre-recording signal strength information from multiple base stations providing an overlapping propagation map within an area of interest. These systems compare real measurements with pre-recorded propagation maps to approximate user location.

In general, the downside of location systems using range-based methods is that they may require additional infrastructure, which increases their price and feasibility. Besides, they can be very sensitive to environmental conditions. Distance estimates obtained by observing signal attenuation may have extreme inaccuracies, due to signal propagation problems, such as the increase of path loss in presence of obstacles, multi-path propagation impairments, co-channel interference and noise disturbances. Location systems based on signal propagation delays, may also require a more precise synchronization technique, which may increase costs and complexity. In addition, if node mobility is involved, wireless channel conditions may be expected to vary widely. Node mobility thus imposes more challenges on location systems.

On the other hand, connectivity-based methods (also known as range-free methods), e.g., [15] and [16], only depend on connectivity conditions. Node connectivity is ensured as long as nodes are located within their common vicinity (i.e., they must be found someplace within the coverage zones of the others). If that is the case, each pair of nodes will be separated at the most by their maximum transmission range. If the number of hops separating a pair of nodes can be determined by indirect measurements using a distance-vector algorithm, for instance, then a set of rough distance estimates can be generated. Given such a set, node location can be solved through the use of analytical methods. Most of these solutions require some nodes be placed at known positions, called *anchors*, in order to set up a coordinate reference system that can establish absolute positions. Works in [17], [18], [19] and [20], for example, make use of this approach, where data analysis is made by an algorithm called multidimensional scaling (MDS) for node position estimation in wireless networks.

It is also usually assumed that nodes are capable of determining the physical location from all other nodes in the network. Unfortunately, in some cases, there are nodes that are not equipped with location devices, they are situated at places where the location system does not work properly or they are disconnected from the wireless network. The combination of all these factors may prevent a node from obtaining location information. In [21], the authors propose an opportunistic ad hoc localization algorithm called urban pedestrian localization (UPL), for estimating the location of mobile nodes in urban districts where such problematic factors may be found.

Recently, some pieces of research have presented different methods that, like DoE, take advantage of node mobility in wireless networks for a variety of purposes. For instance, there are some proposals that use mobile nodes as active data carriers to collect and deliver data packets through large or sparse wireless networks, e.g., [22]. In [23], [24] and [25], the authors show that node mobility can be exploited to disseminate information about the position of destinations without incurring in an excessive signaling communication overhead.

Google Maps [26] is a popular location system for mobile users. In this system, users can obtain accurate location information from a GPS receiver, if such a device is available. Otherwise, Google Maps can infer location information from nearby wireless networks or cell sites. The location of a wireless network or a cell site is determined by using databases available online. The user's location is deduced by discovering which are the nearby cell transmitters or Wi-Fi hot-spots, and retrieving their location from such databases. The downside of Google Maps, or similar location services, is the necessity of Internet connections providing access to the database querying service. Besides, this location system does not offer information about the wireless resources not stored in such databases.

DoE emerges as a novel alternative to other location methods and systems. This is due to the fact that DoE is not based on conventional location techniques, Internet connections, distributed databases or add-on location hardware to work properly. In the following section, we formally present our proposal.

3 Direction of Encounter

DoE is an alternative method to locate static nodes and guide mobile nodes in a wireless network without the use of specialized location hardware, e.g., a GPS receiver. In contrast to other location methods, DoE takes advantage of node mobility and involves only node detection performed by mobile nodes. While crossing a region of interest, mobile nodes implementing DoE can estimate the position of recently found static nodes. Such positions are referenced to the trajectories described by mobile nodes. Based on such position estimates, a mobile node is able to determine the relative position and direction where a specific static node is found. Details about how DoE works appear below.

3.1 DoE Assumptions

The DoE algorithm assumes a wireless network formed by a collection of static nodes randomly scattered over a certain outdoor region. From time to time, this region is visited by mobile nodes. Mobile nodes implementing DoE are also assumed to be capable of detecting and identifying static nodes using the same wireless technology as long as they are within range. In DoE, mobile nodes must be able to determine both where they are located and when the *first* and *last encounter* with a static node occurred. Performing this task depends closely on the *mobility behavior* of mobile nodes. In this respect, DoE can operate under two different modes named *general* and *grid*, both of which will be discussed below and evaluated in the performance evaluation section of this paper.

General mode: In this mode of operation, DoE considers that mobile nodes are free to move following arbitrary trajectories at variable speeds. In this case, the use of an inertial navigation system is mandatory for mobile nodes to establish their positions with respect to their own trajectories. Inertial navigation systems, e.g., [27] and [28], involve the use of a variety of sensors, such as accelerometers, gyroscope sensors or digital compasses, which are now available in many mobile devices (an example of such a system is presented in Section 4.2).

Grid mode: In this mode of operation, DoE considers that mobile nodes move along rectilinear trajectories at a roughly constant speed, which is commonly the case in a grid-type scenario (i.e., a Manhattan-like layout). In this mode, a rectilinear trajectory assumption simplifies the computation of the position of mobile nodes with respect to their own trajectories. It is worth mentioning that in this case DoE achieves this task without the use of any additional hardware other than the wireless radio transceiver. Assuming a grid mode in cases where mobile nodes do not move at a constant speed nor follow rectilinear trajectories will certainly introduce static node position estimation errors. Despite these drawbacks, in addition to the general mode, throughout the paper we discuss this mode in detail because it allows a relatively easy implementation of DoE.

With regard to other assumptions concerning both modes of operation, DoE considers the transmission range to be constant, thus leading to circular coverage zones. Later on, in Section 4.1, we relax this assumption in order to consider more realistic propagation conditions. In the computer simulations, the wireless transmission range of nodes is assumed to be a random variable with normal distribution. We also carried out a series of experiments with a prototype system in order to assess the effects of real propagation conditions. It is expected that variations of the transmission range will lead to location estimation errors.

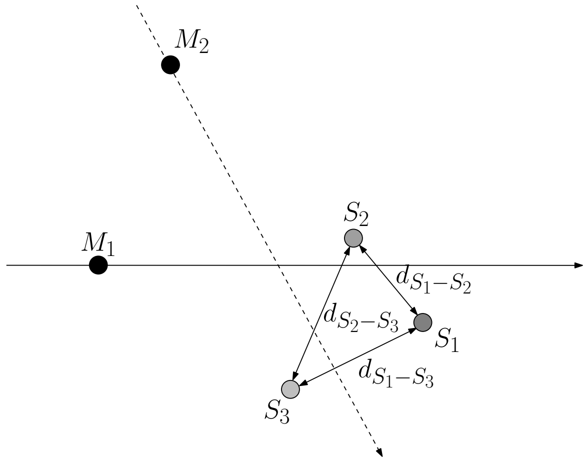

Fig. 1. An example of a wireless network formed by three static nodes (S_1, S_2 and S_3) and two mobile nodes (M_1 and M_2).

Finally, the DoE algorithm relies on a collaborative approach among mobiles nodes to perform its core functions. In the rest of this section we detail the different procedures involved in DoE.

3.2 Node Detection

In order to understand DoE operation, we use a notation that differentiates static nodes from mobile nodes. According to this notation, a set of N static nodes will be represented by $\mathbb{S} = \{S_n \mid n = 1, 2, \ldots, N\}$ and a collection of M mobile nodes will be denoted by $\mathbb{M} = \{M_m \mid m = 1, 2, \ldots, M\}$. Fig. 1 illustrates a simplified example of a network comprised of three static nodes, i.e., S_1, S_2 and S_3. In two arbitrary moments, this network is visited by mobile nodes M_1 and M_2. This figure also depicts the paths followed by both mobile nodes as they travel across this region. The relative distances between each pair of static nodes are also presented in Fig. 1. Let us refer to such distances as *inter-node distances*, which are denoted by $d_{S_i-S_j}$, where $S_i, S_j \in \mathbb{S}$, $i \neq j$.

DoE operation is based on the foundation that mobile nodes crossing a network are capable of detecting the current presence and subsequent absence of static nodes within their coverage zones (*node detection*). These events define the *first* and *last encounter times* between a mobile and a static node. Such instants occur when both nodes are in and out of reach, respectively.

In order to detect static nodes, and depending on the technology being used, DoE may or may not involve the exchange of request and reply messages among mobile and static nodes. In this work, we assume that by setting up their wireless network interfaces in monitor mode, mobile nodes are allowed to detect and identify all traffic transmitted from nearby wireless sources. This is so, since even wireless interfaces that may be apparently inactive, are commonly transmitting or replying to periodic beacons, thus making their detection possible.

Figs. 2a and 2b illustrate the application of DoE in both modes of operation. The former corresponds to the general mode, where the path and speed of mobile node M_m

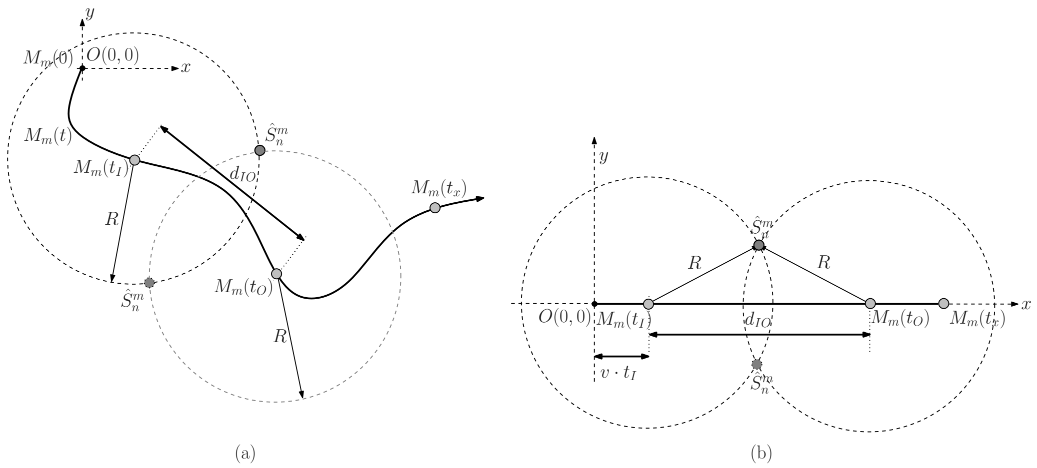

Fig. 2. First and last encounter between mobile node M_m and static node S_n. Geometric solutions for the position of node S_n ($\hat{S}_n^m$). (a) General mode of operation considering an arbitrary trajectory; (b) Grid mode of operation considering a rectilinear trajectory.

are both arbitrary (see Fig. 2a). In this case, the node movement is described by a set of points, $M_m(t) = (X_m(t), Y_m(t))$, lying on the Cartesian Plane (XY). This collection of points can be determined by means of an inertial navigation system. The latter corresponds to the grid mode, where nodes M_m follow rectilinear trajectories at a constant speed (v) (see Fig. 2b). In Figs. 2a and 2b, the origin of the coordinate system is placed at point $O(0,0)$, where mobile node M_m was located when it started to move, i.e., $t = 0$. In Fig. 2b, the horizontal axis of the coordinate system coincides with the path followed by mobile node M_m. For both cases, while traversing the network, mobile nodes must be capable of collecting and storing information about the points where the *first* and *last encounter* with static nodes occurred. Let us denote such points by $M_m(t_I) = (X_m(t_I), Y_m(t_I))$ and $M_m(t_O) = (X_m(t_O), Y_m(t_O))$, respectively. Such points are referenced to the trajectories described by mobile node M_m and their coordinates correspond to the centers of two circles with radius R, i.e., the wireless transmission range.

From now on, the estimated position of static node S_n will be denoted by $\hat{S}_n^m$. In this notation, subindex n indicates which static node has been detected in particular and superindex m specifies which mobile node detected it. In most cases, the estimated position $\hat{S}_n^m$ will have two geometric solutions. These points are situated either at a *left-side position* or at a *right-side position* with respect to the trajectory of node M_m, see Figs. 2a and 2b. Let us represent both solutions by two pairs of coordinates $(\hat{X}_n^m, \hat{Y}_n^m)$. These solutions are determined by computing the intersection points of two overlapped circles of radius R, centered at the points $M_m(t_I)$ and $M_m(t_O)$, respectively. The coordinates of such points are referenced to the mobile node trajectory and are also represented in Figs. 2a and 2b. For the general mode of operation, the geometric solutions for the estimated position $\hat{S}_n^m$ are given by:

$$\hat{X}_n^m = \frac{X_m(t_O) + X_m(t_I)}{2} \mp \frac{Y_m(t_O) - Y_m(t_I)}{d_{IO}} \sqrt{R^2 - \left(\frac{d_{IO}}{2}\right)^2}, \tag{1}$$

and

$$\hat{Y}_n^m = \frac{Y_m(t_O) + Y_m(t_I)}{2} \pm \frac{X_m(t_O) - X_m(t_I)}{d_{IO}} \sqrt{R^2 - \left(\frac{d_{IO}}{2}\right)^2}, \tag{2}$$

where, the term d_{IO} found in Eqs. (1) and (2) corresponds to the distance measured from point $M_m(t_I)$ to point $M_m(t_O)$, i.e., $d_{IO} = \sqrt{(X_m(t_O) - X_m(t_I))^2 + (Y_m(t_O) - Y_m(t_I))^2}$, as shown in Fig. 2a.

For the grid mode, there are some special conditions that need to be taken into consideration. First, according to the coordinate system used in this case, the ordinates of node M_m do not change as time passes, i.e., $Y_m(t_I) = Y_m(t_O) = 0$. Second, the abscissas of node M_m, i.e., $X_m(t_I)$ and $X_m(t_O)$ are simple to obtain by means of: $X_m(t_I) = v \cdot t_I$ and $X_m(t_O) = v \cdot t_O$, respectively. The terms t_I and t_O correspond to the instants in which the *first* and *last encounter* occurred, respectively. After considering such conditions in Eqs. (1) and (2), the geometric solutions for the estimated position $\hat{S}_n^m$ can be easily obtained by:

$$\hat{X}_n^m = \frac{X_m(t_O) + X_m(t_I)}{2} = \frac{v}{2}(t_I + t_O) \tag{3}$$

and,

$$\hat{Y}_n^m = \pm\sqrt{R^2 - \left(\frac{d_{IO}}{2}\right)^2}, \tag{4}$$

where, the term $\frac{d_{IO}}{2}$ found in Eq. (4) corresponds to half the distance traveled by node M_m during the encounter period with a static node S_n. The encounter period, represented by t_{IO}, is the elapsed time between the instants in which *first* and *last encounter* occurred, i.e., $t_{IO} = t_O - t_I\,; t_O > t_I$. Therefore, the distance traveled during the encounter period can be found by: $d_{IO} = v \cdot t_{IO} = v\,(t_O - t_I) = X_m(t_O) - X_m(t_I)$. In this case, if nodes move at variable speeds, the constant speed (v) can be replaced by their average speed of movement, which can be measured or estimated empirically.

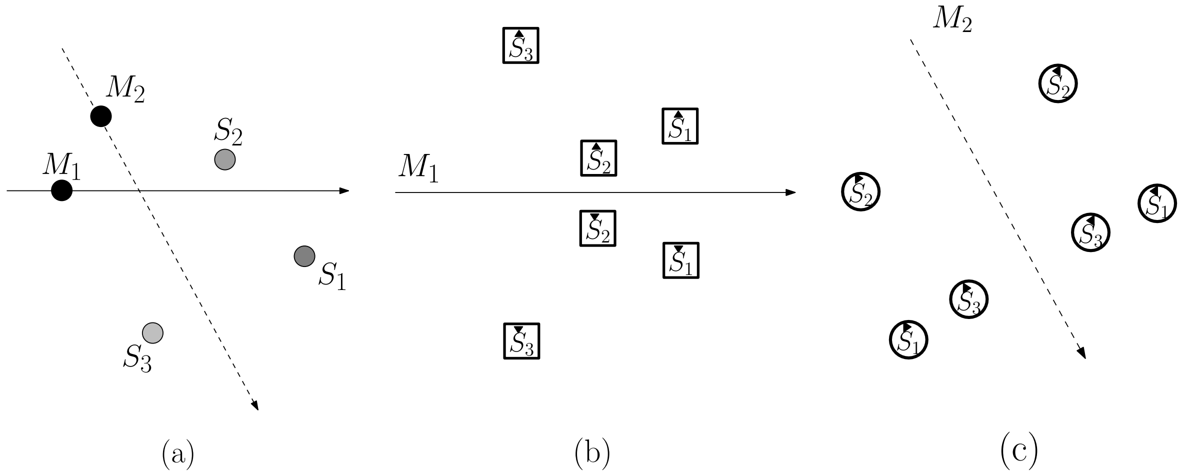

Fig. 3. (a) A wireless network formed by three static nodes, S_1, S_2 and S_3 and two mobile nodes (M_1 and M_2), (b) *Constellation* obtained by mobile node M_1, (c) *Constellation* obtained by mobile node M_2.

Figs. 2a and 2b show the two possible geometric solutions for the estimated position $\hat{S}_n^m$. Such positions are deduced by node M_m, by using Eqs. (1) and (2) for the general mode of operation or Eqs. (3) and (4) for the grid mode. However, this can be done only after the last detection of node S_n occurred, i.e., at a later time $t = t_x$, where $t_x > t_O$. In both cases, the *left-side point* corresponds to the real position of node S_n and the *right-side point* corresponds to a mirrored position. Initially, the position of any static node would involve a position-ambiguity.

We close this subsection by emphasizing that the distinction between the grid and general modes of operation is relevant only to the node detection procedure. The mode of operation does not have any impact on subsequent DoE procedures.

3.3 Constellation Creation

Now, let us define a *constellation* as the collection of estimated positions for a set of static nodes S_n by computing their coordinates using Eqs. (1) and (2) or Eqs. (3) and (4). While traversing a region, node M_m will detect its neighboring nodes and perform the discovery process of its own *constellation* (*constellation* creation). Each mobile node would obtain a different *constellation* depending on its own trajectory. For a node M_m, a *constellation* is a collection of pairs of coordinates $(\hat{X}_n^m, \hat{Y}_n^m)$ which define the two possible geometric solutions associated with $\hat{S}_n^m$. On each *constellation*, there are two combinations or subsets of geometric solutions for the estimated static node positions. One of these subsets will contain the *real positions* and the other one will contain only *mirrored positions*. At this point, there are a few or even no practical ways to determine, by means of a single mobile node, which solutions correspond to the *real-positions* subset and which ones belong to the *mirrored-positions* subset. The following section describes a way to separate real from mirrored positions.

It is also important to note that once a mobile node establishes its own *constellation* of static nodes, DoE no longer needs the information regarding its trajectory. In fact, the DoE algorithm takes as input one or more *constellations* to operate properly without needing to know the underlying trajectory of mobile nodes generating such *constellations*.

3.4 Dealing with Position Ambiguities

In this section we explain how DoE deals with position ambiguities. For simplicity we illustrate this procedure by considering the grid mode, however, we emphasize that exactly the same procedure applies to the general mode of operation.

In order to differentiate, in our explanations, the *left-side* and *right-side* positions of static node S_n discovered by mobile node M_1, we use the following notation: $\overset{\blacktriangle}{\hat{S}}{}_n^1$ and $\overset{\blacktriangledown}{\hat{S}}{}_n^1$, respectively. In turn, the *left-side* and *right-side* positions of static node S_n discovered by mobile node M_2 are represented by $\overset{\blacktriangleleft}{\hat{S}}{}_n^2$ and $\overset{\blacktriangleright}{\hat{S}}{}_n^2$, respectively.

Fig. 3a depicts a wireless network comprised of three static nodes, S_1, S_2 and S_3 and visited by two mobile nodes (M_1 and M_2). Figs. 3b and 3c describe two *constellations* obtained by nodes M_1 and M_2, as they travel across the wireless network. Note that in the simple cases depicted in the figures in this section, squares and circles are used to identify the mobile nodes.

A mobile node may exchange its discovered *constellation* with other mobile nodes found during its journey. Mobile nodes can perform this process by periodically announcing their presence and the availability of their *constellation* to other mobile nodes by emitting some specific messages (i.e., *DoE-Messages*). A *DoE-Message* includes critical information such as the mobile and static node identifications, *constellation* size and position estimates.

At least two *constellations* are required in order to separate the geometric solutions for the static node estimated positions. Therefore, mobile nodes have to cooperate by exchanging their own *constellations* when they meet other mobile nodes that have visited the same area. After a pair of mobile nodes has exchanged their *constellations*, the following procedures can take place.

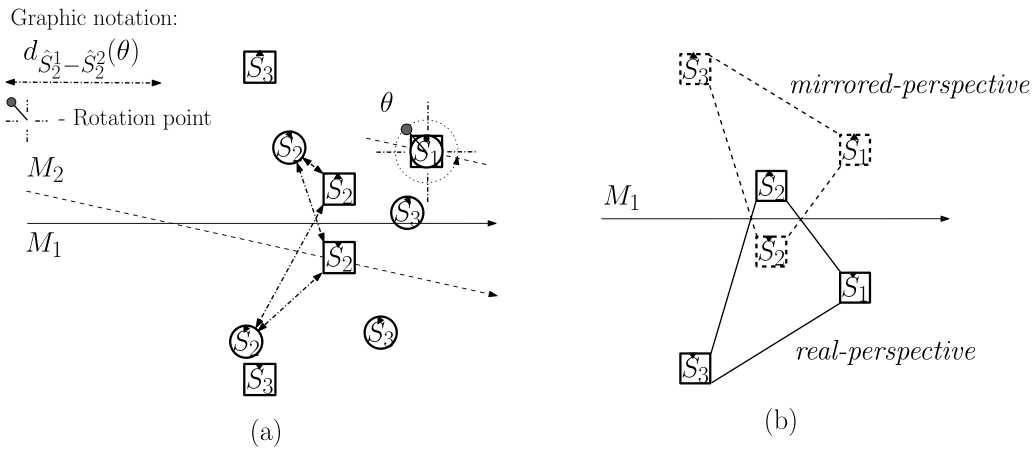

Fig. 4. (a) *Intra-node distances* for node S_2, ($d_{\hat{S}_2^1-\hat{S}_2^2}(\theta)$), represented by dash-dotted lines with arrow-heads at both ends. (b) Two separated subsets of geometric solutions for static nodes S_1, S_2 and S_3, based on the *constellation* obtained by mobile node M_1.

3.5 Constellation Superimposition, Translation and Rotation

- *Constellation superimposition*. When a mobile node has two *constellations*, a *constellation-pair* is generated where all static node position-pairs from one *constellation* are coupled and superimposed with position-pairs on the other *constellation*.
- *Constellation translation*. A reference node must be selected from the *constellation-pair*. Both *constellations* are then centered with respect to the selected reference node. This step causes a position translation for all static nodes. Two possible options are associated with the estimated positions of every static node on each *constellation*, i.e., $\overset{\blacktriangle}{\hat{S}}{}^1_n$ or $\overset{\blacktriangle}{\hat{S}}{}^1_n$ and $\overset{\blacktriangleleft}{\hat{S}}{}^2_n$ or $\overset{\blacktriangleright}{\hat{S}}{}^2_n$. Consequently, four alternatives must be considered and tested as reference node in this step. For instance, if node S_1 is selected as the reference node, the alternatives to be considered are: 1) $\overset{\blacktriangle}{\hat{S}}{}^1_1$ with $\overset{\blacktriangleleft}{\hat{S}}{}^2_1$; 2) $\overset{\blacktriangle}{\hat{S}}{}^1_1$ with $\overset{\blacktriangleright}{\hat{S}}{}^2_1$; 3) $\overset{\blacktriangledown}{\hat{S}}{}^1_1$ with $\overset{\blacktriangleleft}{\hat{S}}{}^2_1$ and 4) $\overset{\blacktriangledown}{\hat{S}}{}^1_1$ with $\overset{\blacktriangleright}{\hat{S}}{}^2_1$. Fig. 4a shows the *constellation-pair* which corresponds to the first case only. In this figure, the *constellations* obtained by mobile nodes M_1 and M_2, shown separately in Figs. 3b and 3c, are then combined to generate this *constellation-pair*.
- *Constellation rotation*. Once a *constellation-pair* is centered on one reference node (rotation point), then one *constellation* is kept fixed and the other one must be gradually rotated. The gradual rotation is intended to determine the best angle at which all static nodes in one *constellation* get the closest to the same static nodes in the other *constellation*. Let us refer to the spacing between two estimated positions of the same static node in two *constellations* as *intra-node distance*. This spacing is obtained by mobile nodes M_k and M_l, e.g., $\hat{S}^k_n$ and $\hat{S}^l_n$. Let us denote such *intra-node distances* by $d_{\hat{S}^k_n-\hat{S}^l_n}(\theta)$.
- *Intra-node distance computation*. Due to the fact that there are two possible positions in each *constellation* for each estimated position, we need to consider four *intra-node distances* that need to be computed in order to find their minimum values. Fig. 4a depicts the four *intra-node distances* for $\hat{S}_2$ at a certain rotation angle θ, i.e., $d_{\hat{S}_2^1-\hat{S}_2^2}(\theta)$.

In order to estimate the proper rotation angle (Θ) at which one *constellation* should be rotated with respect to the other, the square value of the *intra-node distances* must be computed for each θ value. Due to the fact that there are two possible positions for each static node on each *constellation*, it will be necessary to compute four *square intra-node distances*. This computation is performed for each static node, by means of:

$$d^2_{\hat{S}^k_n-\hat{S}^l_n}(\theta) = \left(\hat{X}^k_n(0) - \hat{X}^l_n(\theta)\right)^2 + \left(\hat{Y}^k_n(0) - \hat{Y}^l_n(\theta)\right)^2, \quad (5)$$

where, the pair (k, l) represents the four combinations, i. e., $(k, l) \in \{(\overset{\blacktriangle}{\hat{S}}{}^k_n, \overset{\blacktriangleleft}{\hat{S}}{}^l_n); (\overset{\blacktriangle}{\hat{S}}{}^k_n, \overset{\blacktriangleright}{\hat{S}}{}^l_n); (\overset{\blacktriangle}{\hat{S}}{}^k_n, \overset{\blacktriangleleft}{\hat{S}}{}^l_n); (\overset{\blacktriangle}{\hat{S}}{}^k_n, \overset{\blacktriangleright}{\hat{S}}{}^l_n)\}$.

The coordinate pairs $(\hat{X}^k_n(0), \hat{Y}^k_n(0))$, $(\hat{X}^l_n(\theta), \hat{Y}^l_n(\theta))$, found in Eq. (5), represent the estimated positions of static node S_n obtained by mobile nodes M_k and M_l, respectively. This notation is also intended to differentiate the estimated positions for each static node obtained by both mobile nodes, one position is placed on the *right-side* and the other is placed on the *left-side* of each trajectory. It is worth emphasizing that the second *constellation* is rotated by an angle θ, in an anti-clockwise direction over the first one, which remains fixed (i.e., 0 degree). Then, the algorithm selects the *intra-node distance* with the minimum value, i.e.,

$$d^2_{\underset{min}{\hat{S}_n}}(\theta) = min\left(d^2_{\hat{S}^k_n-\hat{S}^l_n}(\theta)\right). \quad (6)$$

In order to find the best rotation angle at which the *intra-node distances* for all static nodes reach their minimum value, the sum of minimum square *intra-node distances* for all static nodes in a *constellation-pair* ($D^2(\theta)$) should be computed by means of:

$$D^2(\theta) = \sum_{n=1}^{N} d^2_{\underset{min}{\hat{S}_n}}(\theta). \quad (7)$$

Due to symmetry conditions, the sum of minimum square *intra-node distances* for all static nodes computed

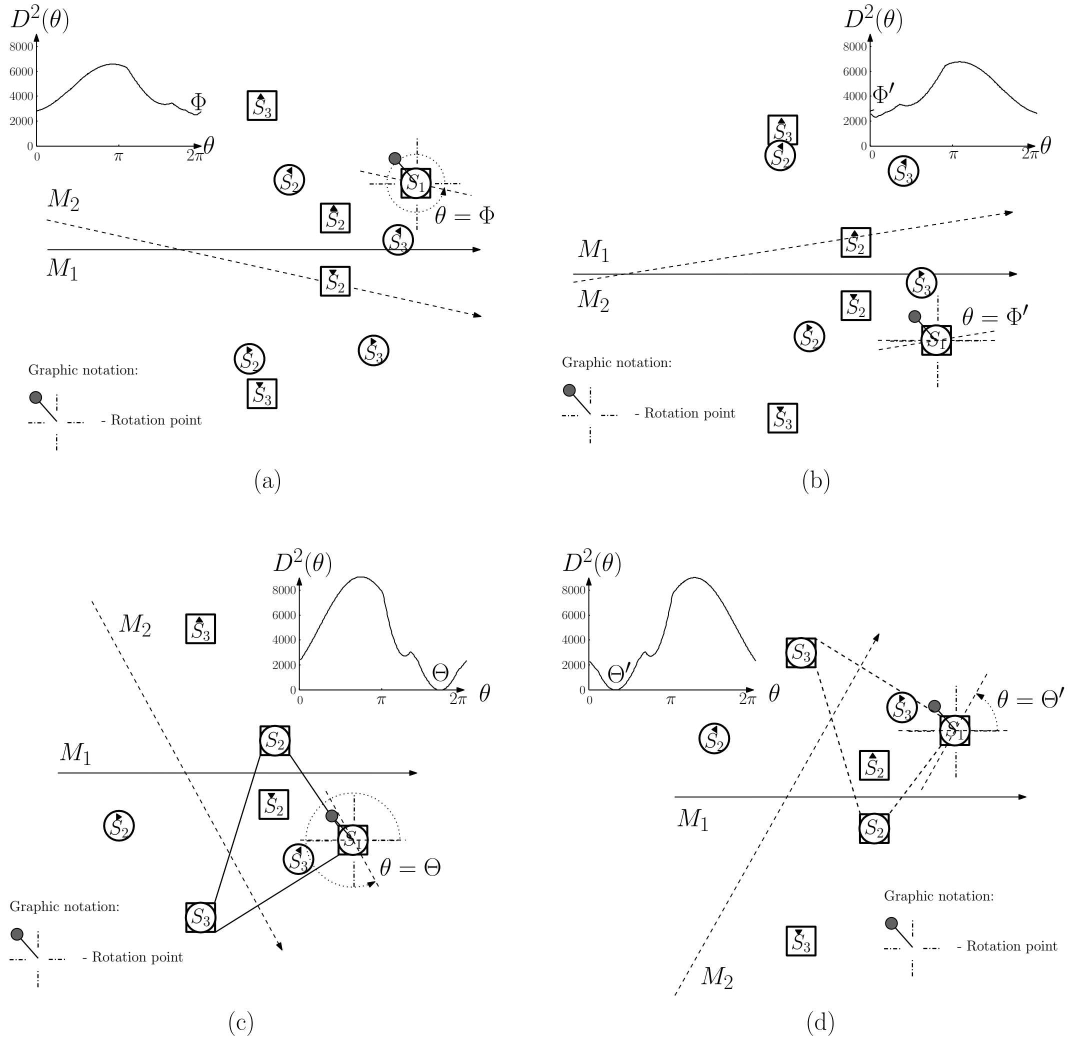

Fig. 5. Procedures of superimposing, translating and rotating two *constellations* obtained by mobile nodes M_1 and M_2 using the four choices for the reference node (S_1) and four different rotation angles.

by the algorithm, i.e., $D^2(\theta)$, will reach its minimum value at two rotation angles. One of these angles corresponds to $\theta = \Theta$. This case occurs when both real positions of the reference node are chosen. The other angle corresponds to its conjugate, i.e., $\theta = \Theta' = 2\pi - \Theta$, which occurs when the two mirrored positions of the reference node are selected. There is a special case where both angles are the same, i.e., $\Theta = \Theta' = \pi$. This happens only when mobile nodes cross over the exact position of the reference node, which also produces a single estimated position for the reference node.

Once the best value for θ has been found, i.e., the one in which $D^2(\theta \approx \Theta) \approx D^2_{min}$ (ideally, $D^2_{min} = 0$), two *sub-constellations* with two graphical representations or maps are generated. Fig. 4b shows the two possible collections of positions for static nodes S_1, S_2 and S_3 which are based on the *constellation* obtained by mobile node M_1 (see the solid line (*real-perspective*) and the dashed line (*mirrored-perspective*) in Fig. 4b. Each map separates a subset of geometric solutions for static nodes in the network.

Figs. 5a, 5b, 5c and 5d show the *constellation-pairs* obtained when the *constellation* discovered by node M_2 is superimposed, centered and rotated with respect to the *constellation* found by node M_1. On each figure, one of the four choices for the reference node is considered. In this example, node S_1 is used as the reference node and rotation point (see the pin and dash-dotted crosses located on the estimated positions of node S_1). On one hand, Figs. 5a and 5b present two combinations for the estimated positions $\hat{S}_1^m$, i.e., mirrored with real positions ($\overset{\blacktriangle}{\hat{S}}{}_1^1$ with $\overset{\blacktriangleleft}{\hat{S}}{}_1^2$) and real with mirrored positions ($\overset{\blacktriangle}{\hat{S}}{}_1^1$ with $\overset{\blacktriangleright}{\hat{S}}{}_1^2$), and two rotation angles, Φ and Φ', respectively. On the other hand, Fig. 5c shows a third case where the right options for reference node S_1 are selected, i.e., ($\overset{\blacktriangledown}{\hat{S}}{}_1^1$ with $\overset{\blacktriangleleft}{\hat{S}}{}_1^2$) and the rotation angle is Θ. Finally, Fig. 5d presents the fourth combination for the estimated position of node S_1, i.e., ($\overset{\blacktriangledown}{\hat{S}}{}_1^1$ with $\overset{\blacktriangleright}{\hat{S}}{}_1^2$) and the rotation angle is Θ', i.e., the conjugate of Θ.

In Figs. 5a, 5b, 5c and 5d, next to each *constellation-pair*, there is a graph plotting the behavior of the sum of minimum square *intra-node distances* for the corresponding *constellation-pair* ($D^2(\theta)$), while the rotation angle θ changes. It

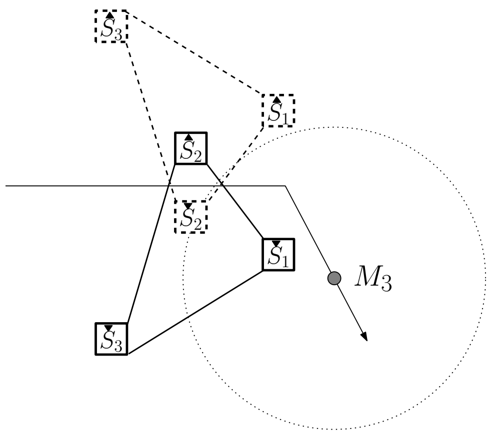

Fig. 6. Identification of the real subset (solid-line triangle) and mirrored subset (dashed-line triangle) when a mobile node (M_3) changes trajectory.

can also be observed that on each graph, $D^2(\theta)$ reaches different values at quite distinct rotation angles. In particular, in Figs. 5c and 5d, we can observe that, when the rotation angle (θ) equals the value of Θ or its conjugate Θ', respectively, $D^2(\theta)$ reaches a minimum value. As a result, a *mirror-free constellation* is generated, such as the one shown in Fig. 4b. On a *mirror-free constellation*, the estimated *inter-node distances* are expected to be similar to the real ones.

From this point on, we will only show the results observed from the *real-perspective*. At a later time, one of the mobile users will be expected to be able to discard the *mirrored-perspective*. This can be done after a mobile node changes its trajectory. After turning to one side, the *right-side*, for example, if a static node is still detected, it can be assumed that the correct *constellation* will be the one indicating that this particular node is on the *right-side*. This procedure is illustrated in Fig. 6. In this figure, a mobile node (M_3) can be observed to follow a horizontal trajectory and then move to its *lower-right side*. Upon reaching a certain point during its movement, node M_3 still detects node S_1 because it remains within its coverage zone (circle of radius R). Therefore, it can be inferred that S_1 must be located at the *right-side* of its previous trajectory. As a consequence, the set that represents the static nodes' real positions will be the one marked with a solid-line and the other one can be discarded. Mobile users equipped with specialized hardware (inertial sensors, such as accelerometers, gyroscopes or solid-state compasses) can carry out this procedure to easily discriminate the *real* from the *mirror-constellations*. Otherwise, a user should manually indicate the trajectory change. We emphasize that the process of removing the *mirror-constellations* is carried out once by a single node on behalf of all nodes in the same region. This procedure eliminates position ambiguities as nodes spread the information about the *mirror-free constellation* to other mobile nodes.

3.6 Dealing with Non-Ideal Conditions

Up to this point, the wireless transmission range has been considered constant for all nodes. Under this assumption, a *mirror-free constellation* provided by DoE will represent the static nodes' final position arranged with a particular distribution. In such node arrangement, the estimated *inter-node distances* among all nodes are expected to be as close as possible to their real *inter-node distances*. Ideal conditions make it possible that only a pair of mobile nodes be required while implementing DoE to obtain an accurate map of static nodes in their neighborhood.

Under real conditions, each node would have a different transmission range due to a variety of signal fluctuations. These fluctuations are caused by many factors, such as signal propagation impairments along different paths. In order to capture such variability, we consider more realistic scenarios where the wireless transmission range is a random variable R_m with a probabilistic distribution, for example, a normal distribution, i.e., $R_m \sim N(R, \sigma_R^2)$. Such conditions introduce an error in the location method which makes it necessary that more than a pair of mobile nodes cooperate to estimate the static node positions and reduce location errors.

In this work, we consider that the mean value of the random variable R_m is the same nominal value used in the computation of estimated positions by DoE (see the term R in Eqs. (1), (2) and (4)). On one hand, the wireless transmission range determines when the *first* and *last encounter* between a pair of nodes occurred. On the other hand, node mobility mainly defines the encounter period between mobile and static nodes. In particular, under grid mode operation, there may be discrepancies between the real and estimated distances traveled by mobile nodes, which increases the position estimation error.

Now, let us consider that M mobile nodes travel across a region at different times. By sharing the information contained in their M *constellations*, these nodes contribute to improve the estimated positions and *inter-node distances* provided by DoE. An improved position estimate can be obtained by computing the average position from a finite set of points, as shown in [29], [30]. The result of averaging the estimated positions of M views of the same static node can be described as a *centroid* which represents their mean spatial point. In this case, if the number of points is M, the centroid for node S_n, denoted by $\overline{S}_n^M$ will be given by:

$$\overline{S}_n^M = \frac{1}{M}\sum_{m=1}^{M} \hat{S}_n^m, \tag{8}$$

where, the term $\hat{S}_n^m$ is the estimated position of node S_n deduced by node M_m.

As more mobile nodes cross the network, more position estimates will be computed, thus originating a larger collection of positions that can be used to calculate a better centroid. The $(M+1)$st mobile node traversing a region can compute a new centroid, given by $\overline{S}_n^{M+1}$, using the previous centroid $\overline{S}_n^M$, obtained by averaging M samples, and the recently estimated position of node S_n, defined by $\hat{S}_n^{M+1}$, i.e.,

$$\overline{S}_n^{M+1} = \frac{1}{M+1}\left(M\overline{S}_n^M + \hat{S}_n^{M+1}\right), \tag{9}$$

where, the term $\hat{S}_n^{M+1}$ is the estimated position of node S_n deduced by node M_{M+1}. Consequently, while exchanging *constellations*, mobile nodes must report not only the centroid computation, but also the number of points involved in such computation. Mobile nodes exchanging *constellations* must take this number into account in order to make

TABLE 1
Operation Count for DoE Core Procedures Considering a *Constellation Size* of N Static Nodes

Procedure	Operation count (flops)
a) Detection of N static nodes	$24N$ or $9N$
b) Constellation translation	$2N$
c) Constellation rotation	$10(N-1)$
d) Intra-node distance computations	$20(N-1)$
e) Minimum intra-node distances	$3(N-1)$
f) Sum of minimum square intra-node distances (Eq. (7))	$(N-1)$

a weighted calculation of the new centroid, as the one described by Eq. (9).

Instead of offering precise location information of static nodes (absolute coordinates), DoE provides mobile nodes with information about the static nodes' relative positions and *inter-node distances*. DoE performance can be evaluated by computing the mean absolute error of distance estimates ($\overline{E}$) by averaging the differences between the real and estimated *inter-node distances* for all pairs of static nodes, i.e.,

$$\overline{E} = \frac{1}{Q}\sum_{q=1}^{Q}\left| d_{S_i - S_j} - d_{\overline{S}_i^M - \overline{S}_j^M} \right|_q, \tag{10}$$

where, Q is the number of *inter-node distances* among N static nodes, thus $Q = \frac{(N)(N-1)}{2}$. The terms $d_{S_i - S_j}$ are the real *inter-node distances*, measured between a pair of static nodes S_i and S_j. The terms $d_{\overline{S}_i^M - \overline{S}_j^M}$ correspond to the *inter-centroid* distances, which are measured between centroids $\overline{S}_i^M$ and $\overline{S}_j^M$ obtained for these static nodes.

The mean relative error of distance estimates can be computed by means of:

$$\overline{e} = \frac{1}{Q}\sum_{q=1}^{Q}\left| \frac{d_{S_i - S_j} - d_{\overline{S}_i^M - \overline{S}_j^M}}{d_{S_i - S_j}} \right|_q. \tag{11}$$

We could infer that the value of the error may be gradually reduced by incorporating more *constellation pairs*. Nevertheless, once we conducted the simulations and experiments, which are reported in the evaluation section of the DoE algorithm (see Section 4), we concluded that the mean relative error reaches steady state values with just a small number of mobile nodes, i.e., from five to 10 nodes, in typical scenarios.

3.7 Computational Complexity

The complexity of the DoE algorithm can be estimated by counting the number of operations performed in each one of its core procedures. In Table 1, we summarize such numbers considering two *constellations* of N static nodes each.

The operation count in procedure (a) corresponds to the *constellation* discovery process. This count raises $24N$ when the general mode of operation is considered and $9N$ in the grid mode. For both cases, procedures (c)-(f) have to be carried out at each rotation step (K). Therefore, considering the K rotation steps it represents $[10(N-1) + 20(N-1) + 3(N-1) + (N-1)]K = 34(N-1)K$ flops. As previously mentioned in Section 3.5, the *constellation translation* has to consider four possible alternatives for the reference node. Consequently, the total number of operations in these core procedures becomes $136(N-1)K$. It can be observed that the operation count strongly depends on *constellation size* (N) and the number of rotation steps (K).

If the mobile nodes implementing the DoE algorithm have limited computational resources, a practical way to reduce the computational complexity involves two possible alternatives. The former consists of taking just a small subset of nodes in a large *constellation*. By means of simulations, we found that the angle that minimizes the distance error can be reliably estimated with as few as three static nodes. The latter consists of reducing the number of rotation steps. A number of strategies can be implemented to this end. For instance, once an interval containing the minimum has been roughly identified, it can be subdivided into smaller intervals in order to find a more precise rotation angle.

Finally, centroid computations can also be reduced by only considering a small number of mobile nodes. As mentioned before, simulations indicate that with just five to 10 mobile nodes, the DoE algorithm provides acceptable margins of error.

4 DoE Performance Tests

This section analyzes the performance of DoE as a location method by considering three simulation scenarios and two sets of experiments. These tests were conducted to prove DoE's effectiveness and limitations to locate static nodes.

4.1 DoE Simulations

This subsection presents the DoE performance as a location method by considering a set of 300 simulation tests for three scenarios under variable conditions. Such conditions include random transmission ranges R_m with a normal distribution around a mean value of $R = 100$ [m] and considering three standard deviation values $\sigma_R = \{R/100, R/20, R/10\}$ [m], i.e., $R_m \sim N(R, \sigma_R^2)$. In each of these scenarios, the total number of mobile nodes was $M = 100$, each one of them following a rectilinear trajectory in a random direction (grid mode operation). Mobile nodes moved at a constant speed of $v = 1$ [m/s]. In each scenario, the number of static nodes was $N = 3$ (denoted by: S_1, S_2 and S_3). By considering a uniform spatial distribution, static nodes were randomly scattered over a square area of 100×100 m^2, as shown in Figs. 7a, 7b and 7c. Each figure presents one case.

Figs. 7a, 7b and 7c show the centroids' position for the three static nodes, which were all computed by means of Eq. (9). These figures also illustrate the real and estimated *inter-node distances* measured among static nodes S_1, S_2 and S_3. In each figure, the real positions of such static nodes are represented by the symbol $*$. In the same figures, the estimated positions of static nodes $\hat{S}_1^m$, $\hat{S}_2^m$ and $\hat{S}_3^m$ are represented by the symbols $\circledast$, $\diamond$, and $\bigstar$, respectively. The position of their centroids are represented by the symbol $\circ$. Figs. 7a , 7b and 7c also show the sample cumulative distribution function (CDF) for each case. These functions represent the cumulative relative frequency of occurrence of the mean relative error $\overline{e}$. By observing these graphs, it can be deduced that dispersion of $\overline{e}$ is higher as the variability of the wireless transmission range increases, which is captured by a larger standard deviation (σ_R). By observing the CDF of each case, we can deduce that the mean relative error for at least 65 percent of the mobile nodes is below 10, 20 and 30

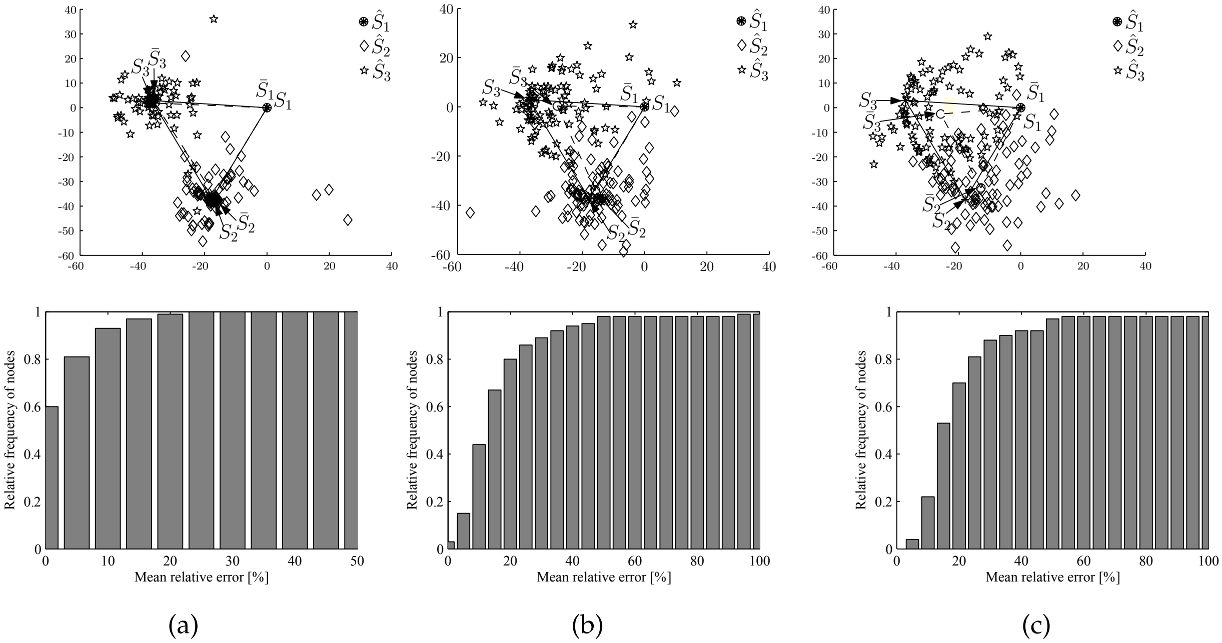

Fig. 7. *Top*, node distribution, centroid positions and *inter-node distances*; *bottom*, cumulative distribution function of the mean relative error ($\bar{e}$) for three cases: (a) $\sigma_R = R/100 = 1$ [m]; (b) $\sigma_R = R/20 = 5$ [m] and (c) $\sigma_R = R/10 = 10$ [m].

percent, while considering the three standard deviation values, i.e., $\sigma_R = \{R/100, R/20, R/10\}$, respectively.

4.2 DoE Experiments

In order to test the performance of DoE as a location method under real conditions, we conducted two sets of experiments. The first one corresponds to the general mode of operation where mobile nodes follow arbitrary trajectories, while the second one considers the grid mode, where rectilinear trajectories are common.

General mode (DoE campus experiment). The first group of experiments consisted of a series of tests intended to estimate the position of five Wi-Fi access points found at the campus of the National Autonomous University of Mexico (UNAM). This region covers an outdoor area of approximately 100×100 m^2. The area is surrounded by a variety of trees and several two or three story buildings. A mobile device, also equipped with a Wi-Fi interface, was carried by a user while walking along the pedestrian pathways in this area. The mobile user followed six different trajectories in both directions, as shown in Fig. 8a.

In order to reconstruct the trajectories followed by the mobile user, as accurately as possible, an inertial navigation system was implemented by means of the accelerometer and gyroscope sensors available in the mobile device. The accelerometer measures speed changes and allowed us to determine whether the user was moving or not (an example is shown in the top part of Fig. 8b). In turn, the gyroscope indicates changes in direction of motion measured with respect to the magnetic North (see the middle part of Fig. 8b). By combining both data, the trajectory can be easily reconstructed (an example is shown in the bottom part of Fig. 8b).

While walking along the pathways, the mobile device collected both inertial sensor data as well as DoE related information. In order to compute the corresponding *constellation* for each trajectory, we measured the wireless transmission range at different places for various APs. Then, these measurements were averaged. The average transmission range obtained from these measurements was about $R = 75$ m. It is worth pointing out that these experiments did not interfere with normal campus activities.

After obtaining the associated *constellations* according to the trajectories followed by the mobile user, the translation and rotation procedures of DoE were applied. The positions of the APs were then estimated and the centroids of each AP were computed. Fig. 8a also depicts the real and estimated positions of five APs. Centroids are indicated by the symbol $\bigcirc$ in Fig. 8a. The mean error between the real and estimated positions of each AP fluctuated between 4 and 12 m, with an average error of 8 m. These errors are mainly due to propagation impairments (created by multipath, reflection, scattering and shadowing effects). However, we consider this error may be acceptable in many practical applications.

Grid mode (DoE urban experiment). The second group of experiments were intended to discover the position of ten Wi-Fi access points found in an urban region in Mexico City. The considered area in these experiments corresponds to a rectangle that approximately measures 250×350 m^2. In this scenario, the streets follow the typical grid-layout (see Fig. 9). Typically, four- to six-story buildings are found in this area, which certainly affects radio propagation. In this set of experiments, we considered an average wireless transmission range of $R = 60$ m. We conducted a similar procedure to the one used in the university campus experiment to measure the wireless transmission range for this scenario. For these experiments, the average speed of movement ($v = 1.2$ m/s) was deduced by estimating the average distance walked by mobile users over their trip time. Mobile users followed six different trajectories, according to the

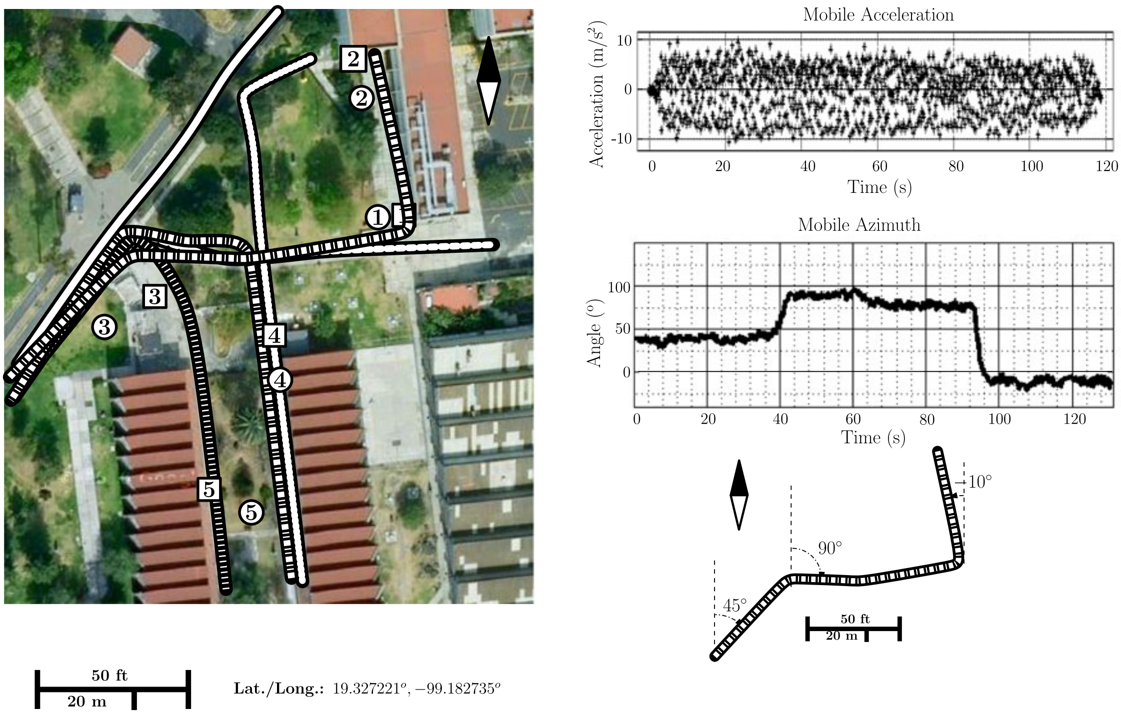

(a) (b)

Fig. 8. (a) Six different trajectories followed by a mobile node. The actual location of five access points is represented by □. Centroids calculated by DoE are indicated by ○. (b) Sensor data related to a mobile node acceleration (top), azimuth (middle) and the reconstructed trajectory (bottom).

street layout in both directions, which accounted for 12 different constellations. It is important to mention that the mobile devices did not have any additional hardware at their disposal other than their Wi-Fi interfaces. These experiments were performed during normal office hours. The users carrying mobile devices followed rectilinear trajectories along the sidewalks, but they occasionally had to stop before crossing a street.

While we found dozens of Wi-Fi sources, we only focused on 10 of them because their locations were identifiable from the streets. In Fig. 9, real and estimated positions of 10 static nodes are represented by □ and ○, respectively. The mean distance error between real and estimated positions of nodes for this set of experiments fluctuated between 6 and 24 m, with an average error of 15 m. While these errors were larger compared to the university campus experiment, we consider it to be good, especially if we take into account the presence of many tall buildings affecting the propagation characteristics, and the fact that mobile devices did not always move at the previously assumed speed.

5 DoE Applications

We believe DoE could have a broader set of applications than many location methods reported in the literature because no other method provides static node location information without involving such nodes in the location process. In addition, DoE is relatively simple to implement. The proposal could practically work in any kind of wireless network as long as there is direct communication among neighboring nodes and node mobility. For the same reasons, we think that DoE would be more suitable for wireless local area networks involving mobile nodes (either infrastructure-based WLANs or MANETs), wireless sensor networks (WSNs) or wireless personal networks (WPANs) deployed in outdoor environments.

Fig. 9. A residential area in Mexico City where the streets follow the typical grid layout.

DoE information may also be used in social networks and location-aware services. In particular, these applications could guide roaming users to places where they can find another person or a service provider in large outdoor sites or open spaces (campuses, stadiums, warehouses, markets, stores, etc.), locate a vehicle in a parking lot or discover some network devices with wireless interfaces (printers, access points, routers, etc.).

In the field of ad hoc networks, DoE information can be used to enhance the operation of flooding, routing and relaying techniques. In other words, location information can be used to: a) demarcate a smaller region of the network where flooding will take place; b) indicate where the destination node is located; or c) select a relaying node that is moving in a direction that is likely to physically reach a node of interest and deliver a message directly. Consequently, DoE could reduce network congestion, especially in large-sized wireless networks with high node density where most related protocols do not scale well.

Another field where DoE information may be used is wireless sensor networks. In WSN, data collected by sensor nodes may be completely irrelevant if no location information is provided. On the other hand, it is common for a WSN to involve a random and dense deployment of sensor nodes, which makes it complex to determine the position of all nodes. Once the sensors have been deployed, DoE could be implemented by one or several mobile nodes only dedicated to estimate the position of each sensor in the network.

6 Conclusions

In this work, we propose an alternative method to locate static nodes in wireless networks. Direction of encounter takes advantage of node mobility and node detection without using traditional location systems or specialized location hardware, such as a GPS receiver. DoE is based on the principle that mobile nodes are able to detect the presence and absence of nearby nodes as they enter or leave their coverage regions. In order to establish the relative position of any neighboring node, mobile nodes must register the instants in which the *first* and *last encounter* with nearby nodes occurred. Mobile nodes can use this information to estimate neighboring nodes' relative position by referencing them to their trajectories (e.g., a specific neighboring node can be placed in a position ahead, behind, left or right from the actual direction of the mobile node). Information about the static node positions is exchanged among mobile nodes. Such information may be used by roaming nodes to estimate the direction where a specific node or a group of nodes can be found. DoE considers two different modes of operation: general and grid. In general mode, mobile nodes are free to move following arbitrary trajectories at variable speeds, in which case the use of an inertial navigation system is required. In grid mode, it is assumed that mobile devices move along rectilinear trajectories at a constant speed, which extends the use of DoE in devices having only a wireless interface. DoE location accuracy has been evaluated by simulations and experiments under a diversity of conditions, such as fluctuations in the wireless transmission range and a variable number of mobile nodes with different trajectories. In general, the results obtained by this evaluation show that DoE exhibits acceptable margins of error for both modes of operation. It is worth pointing out that DoE location accuracy increases as more mobile nodes travel across the area of interest and it reaches steady state with just a few mobile nodes. To the best of the authors' knowledge, this is the first time that node mobility is used as the basis of a location method.

Acknowledgments

This work was supported in part by research funds from CONACyT (105117/105279), DGAPA-PAPIIT (IN108910/IN114813), Texas A&M University-CONACyT (2010-049), PAPIME PE 103807 and PROMEP (12711445; 12711609 and 12711828).

References

[1] Y. B. Ko and N. H. Vaidya, "Location-aided routing (LAR) in mobile ad-hoc networks," in *Proc. 4th Ann. ACM/IEEE Int. Conf. Mobile Comput. Netw.*, Dallas, TX, USA, 1998, pp. 67–70.

[2] D. Niculescu and B. Nath, "Ad-hoc positioning system (APS)," in *Proc. IEEE Global Telecommun. Conf.*, San Antonio, CA, USA, 2001, vol. 5, pp. 2926–2931.

[3] P. Bahl and V. N. Padmanabhan, "RADAR: An in-building RF-based user location and tracking system," in *Proc. IEEE Conf. Comput. Commun.*, Tel Aviv, Israel, 2002, pp. 7–9.

[4] S. Capkun, M. Hamdi, and J. P. Hubaux, "GPS-Free positioning in mobile ad-hoc networks," *Cluster Comput. J.*, vol. 5, no. 2, pp. 157–167, Apr. 2002.

[5] C. Y. Wen, Y. C. Hsiao, and F. K. Chan, "Cooperative anchor-free position estimation for hierarchical wireless sensor networks," *Sensors*, vol. 10, no. 2, pp. 1176–1215, 2010.

[6] L. Wang and Q. Xu, "GPS-Free localization algorithm for wireless sensor networks," *Sensors*, vol. 10, no. 6, pp. 5899–5926, 2010.

[7] R. Marcelin-Jimenez, M. Ruiz-Sanchez, M. Lopez-Villasenor, V. Ramos-Ramos, C. Moreno-Escobar, and M. Ruiz-Sandoval, *A Survey on Localization in Wireless Sensor Networks*. Hershey, PA, USA: IGI Global, 2010.

[8] G. Mao and B. Fidan, *Localization Algorithms and Strategies for Wireless Sensor Networks*. Hershey, PA, USA: IGI Publishing, 2009.

[9] L. M. Pestana and L. M. R. Peralta, "Collaborative localization in wireless sensor networks," in *Proc. Int. Conf. Sens. Tech. Appl.*, Valencia, Spain, Oct. 2007, pp. 94–100.

[10] S. A. Golden and S. S. Bateman, "Sensor measurements for WiFi location with emphasis on time-of-arrival ranging," *IEEE Trans. Mobile Comp.*, vol. 6, no. 10, pp. 1185–1198, Oct. 2007.

[11] P. Uthansakul and M. Uthansakul, "WLAN positioning based on joint ToA and RSS characteristics," *Int. J. Electron., Comm. Comput. Eng.*, vol. 1, no. 3, pp. 395–402, 2009.

[12] R. Yamasaki, A. O. T. Tamaki, N. Matsuzawa, and T. Kato, "TDoA location system for IEEE 802.11b WLAN," in *Proc. IEEE Wireless Comm. Netw. Conf.*, New Orleans, LO, USA, 2005, vol. 4, pp. 2338–2343.

[13] D. Niculescu and B. Nath, "Ad-hoc positioning system (APS) using AoA," in *Proc. IEEE Conf. Comput. Commun.*, San Francisco, CA, USA, 2003, vol. 3, pp. 1734–1743.

[14] T. Kitasuka, K. Hisazumi, T. Nakanishi, and A. Fukuda, "Positioning techniques of wireless LAN terminals using RSSI between terminals," in *Proc. Int. Conf. Pervasive Syst. and Comput.*, Las Vegas, NV, USA, 2005, pp. 47–53.

[15] P. Vicaire and J. Stankovic, "Elastic localization: Improvements on distributed, range free localization for wireless sensor networks," Dept. Comput. Sci., Univ. of Virginia, Tech. Rep. CS-2004-35, 2004.

[16] Y. Shang, W. Ruml, and Y. Zhang, "Localization from mere connectivity," in *Proc. ACM Int. Symp. Mobile Ad Hoc Netw. Comput.*, Annapolis, MD, USA, ACM, Jun. 2003, pp. 201–212.

[17] Y. Shang and W. Ruml, "Improved MDS-based localization," in *Proc. IEEE Conf. Comput. Commun.*, Hong Kong, 2004, pp. 2640–2651.

[18] C. Wu, W. Sheng, and Y. Zhang, "Mobile sensor networks self localization based on multi-dimensional scaling," in *Proc. IEEE Int. Conf. Robot. Autom*, Apr. 2007, pp. 4038–4043.

[19] J. Shu, R. Zhang, L. Liu, Z. Wu, and Z. Zhou, "Cluster-based three-dimensional localization algorithm for large scale wireless sensor networks," *J. Comput., Acad. Publisher*, vol. 4, no. 7, pp. 585–592, 2009.

[20] C. Moreno-Escobar, R. Marcelin-Jimenez, E. Rodriguez-Colina, and M. Pascoe, "A distributed cluster-based localization method for wireless sensor networks," in *Proc. Sixth Int. Conf. Syst. Netw. Commun.*, Barcelona, Spain, 2011, pp. 55–62.

[21] A. Uchiyama, S. Fujii, K. Maeda, T. Umedu, H. Yamaguchi, and T. Higashino, "UPL: Opportunistic localization in urban districts," *IEEE Trans. Mobile Comput.*, vol. 12, no. 5, pp. 1009–1022, May 2013.

[22] R. C. Shah, S. Roy, S. Jain, and W. Brunette, "Data MULEs: Modeling a three-tier architecture for sparse sensor networks," in *Proc. First IEEE Int. Workshop Sens. Netw. Protocols Appl.*, 2003, pp. 30–41.

[23] M. Grossglauser and M. Vetterli, "Locating nodes with EASE: Last encounter routing in ad-hoc networks through mobility diffusion," in *Proc. IEEE Conf. Comput. Commun.*, San Francisco, CA, USA, Mar. 2003.

[24] N. Sarafijanovic-Djukic and M. Grossglauser, "Last encounter routing under random waypoint mobility," in *Proc. Netw. Technol., Serv., Protocols; Performance Comput. Commun. Netw.; Mobile Wireless Commun.*, Athens, Greece, May 2004, pp. 974–988.

[25] M. Grossglauser and M. Vetterli, "Locating mobile nodes with EASE: Learning efficient routes from encounter histories alone," *IEEE/ACM Trans. Netw.*, vol. 14, no. 3, pp. 457–469, June 2006.

[26] R. Gibson and S. Erle, *Google Maps Hacks: Tips & Tools for Geographic Searching and Remixing (Hacks)*. Sebastopol, CA, USA: O'Reilly Media, Inc., 2006.

[27] B. Barshan and H. Durrant-Whyte, "Inertial navigation systems for mobile robots," *IEEE Trans. Robot. Autom.*, vol. 11, no. 3, pp. 328–342, Jun. 1995.

[28] F. Evennou and F. Marx, "Advanced integration of WiFi and inertial navigation systems for indoor mobile positioning," *EURASIP J. Appl. Signal Process*, vol. 2006, pp. 164–164, Jan. 2006.

[29] T. M. Apostol and M. A. Mnatsakanian, "Centroids constructed graphically," *Math. Mag.*, vol. 77, no. 3, pp. 201–210, Jun. 2004.

[30] G. Kang, T. Pérennou, and M. Diaz, "Barycentric location estimation for wireless networks indoors localization," *Int. J. Hybrid Inf. Technol.*, vol. 2, no. 2, pp. 1–12, Apr. 2009.

Michael Pascoe-Chalke received the BSc degree in mechanical-electrical engineering in 1997 and the MSc and PhD degrees with honors in electrical engineering in 2005 and 2010, respectively, all from the National Autonomous University of Mexico (UNAM). His research interests include location systems and cognitive wireless networks. He is currently an associate professor with the Metropolitan Autonomous University (UAM) in Mexico City.

Javier Gomez-Castellanos received the BSc degree with honors in electrical engineering in 1993 from the National Autonomous University of Mexico (UNAM) and the MSc and PhD degrees in electrical engineering in 1996 and 2002, respectively, from Columbia University and its COMET Group. He was at the IBM T.J. Watson Research Center. His research interests cover routing, QoS, and MAC design for wireless ad hoc, sensor, and mesh networks. Since 2002, he has been a full-time professor with UNAM.

Veronica Bonilla-Gonzalez received the BSc degree in telecommunications engineering in 2001 and the MSc degree in electrical engineering in 2012 from the National Autonomous University of Mexico (UNAM). From 2001 to 2012, she was a part-time lecturer at UNAM. From 2001 to 2009, she was at TELCEL as a new services engineer. She is currently a solution specialist at NOKIA Siemens Networks.

Miguel Lopez-Guerrero received the BSc degree in mechanical-electrical engineering in 1995 and the MSc degree in electrical engineering in 1998, both with honors from the National Autonomous University of Mexico. He received the PhD degree in electrical engineering from the University of Ottawa in 2004. He is currently an associate professor with the Metropolitan Autonomous University (UAM) in Mexico City. His academic interests span several areas of networking technology. He is a member of the IEEE.

Victor Rangel-Licea received the BSc (Hons) degree in computer engineering from the National Autonomous University of Mexico (UNAM) in 1996. He received the MSc and PhD degrees from the University of Sheffield, United Kingdom, in 1998 and 2002, respectively. His research focuses on QoS, traffic modeling, and scheduling for mobile broadband wireless access networks. He has been with the School of Engineering (UNAM) since 2002 as a research professor.

Enrique Rodriguez-Colina received the BSc degree in electronics engineering in 1995 and the MSc degree in computer science in 2003 from the Autonomous Metropolitan University (UAM) in Mexico. He received the PhD degree in engineering in 2009 from the University of Cambridge, United Kingdom. He was a research associate at the University of Girona in 2009. He is currently an associate professor at UAM. His research interests are in the area of telecommunications, e.g., cognitive radio networks and wireless sensor networks. He is a member of the IEEE.